TUDelft

Delft University of Technology

A study to improve light confinement and rear-surface passivation in a thin-Cu(In, Ga)Se$_2$ solar cell

Suresh, S.; de Wild, J.; Kohl, T.; Buldu, D. G.; Brammertz, G.; Meuris, M.; Poortmans, J.; Isabella, O.; Zeman, M.; Vermang, B.

Important note
To cite this publication, please use the final published version (if applicable).
Please check the document version above.

A study to improve light confinement and rear-surface passivation in a thin-Cu(In, Ga)Se₂ solar cell

S. Suresh[a,b,*], J. de Wild[c,d], T. Kohl[c,d], D.G. Buldu[c,d], G. Brammertz[c,d], M. Meuris[c,d], J. Poortmans[a,d,e], O. Isabella[b], M. Zeman[b], B. Vermang[c,d]

[a] imec (partner in Solliance & EnergyVille), Kapeldreef 75, Leuven, 3001, Belgium
[b] Photovoltaic Materials and Devices Laboratory, Delft University of Technology, Mekelweg 4, Delft, 2628, CD, the Netherlands
[c] Institute for Material Research (IMO), Hasselt University (partner in Solliance & EnergyVille), Agoralaan gebouw H, Diepenbeek 3590, Belgium
[d] imec division IMOMEC (partner in Solliance & EnergyVille), Wetenschapspark 1, 3590 Diepenbeek, Belgium
[e] Department of Electrical Engineering, KU Leuven, Kasteelpark Arenberg band10, 3001 Heverlee, Belgium

A B S T R A C T

Reducing the absorber layer thickness below 1 μm for a regular copper indium gallium di-selenide (CIGS) solar cell lowers the minimum quality requirements for the absorber layer due to shorter electron diffusion length. Additionally, it reduces material costs and production time. Yet, having such a thin absorber reduces the cell efficiency significantly. This is due to incomplete light absorption and high Molybdenum/CIGS rear-surface recombination [1]. The aim of this research is to implement some innovative rear surface modifications on a 430 nm thick CIGS absorber layer to reduce both these affects: an aluminium oxide passivation layer to reduce the back-surface recombination and point contact openings using nano-particles for electrical contact. The impact of the implementation of all these rear-surface modifications on the opto-electrical properties of the CIGS solar cell will be discussed and analyzed in this paper.

1. Introduction

Recently, power conversion efficiencies of about 22.9% were obtained for small-area copper indium gallium di-selenide (CIGS) solar cells, however they were achieved with absorbers thicker than 1 μm [2]. When compared to CIGS absorbers with a standard thickness of 2–3 μm, sub-micron absorbers limit usage of critical feed-stock (reduced manufacturing costs), reduce the bulk defects (due to reduced bulk volume) and increase the potential for higher manufacturing throughput (reduced deposition times). Yet, for sub-micrometer CIGS solar cells, issues surrounding a highly recombinative rear interface (the electron-hole pair is generated in the vicinity of the back contact) and incomplete absorption of incident solar spectrum (partly due to low reflection at the Molybdenum (Mo) /CIGS interface) limit its usage. The combined effects of the same lead to a reduced open-circuit voltage (V_{OC}) and short circuit current (J_{SC}). One approach to reduce the rear interface recombination for instance would be to use a passivation layer; the passivation layer reduces the interface recombination by field effect and chemical passivation [3]. For a thin-CIGS solar cell, an ultra-thin film of aluminium oxide (Al_2O_3) can be used to passivate the rear interface. The use of an Al_2O_3 layer is justified as 1) first principle calculations by Hsu et al. [4] estimate a 35% reduction in the interface trap density (Mo/CIGS) 2) a built-in field is created due to a high density of fixed negative charge which shields the minority charge

carriers from getting recombined in the rear. Thus, by implementing an Al_2O_3 layer, the surface recombination velocity can be brought down to 100 cm/s (estimated from Solar Cell Capacitance Simulator [5]), leading to an enhanced V_{OC} [5].

As the Al_2O_3 layer is of non-conducting type, point contacts are necessary for electrical connection in the passivated cell. The size and distance between the point contacts (pitch) is determined by, among other parameters, the minority carrier diffusion length. When compared to c-Si solar cells (several hundred micrometers), thin film solar cells like CIGS have very short minority carrier diffusion length, thereby lifetime [6]. Thus, if a diffusion length of 0.5–1.25 μm is feasible, nano-sized openings (a few hundred nanometers in diameter) for a pitch varying from 1.25 to 2.5 μm (scaled from the Si-passivated emitter and rear cell design) is necessary for efficient carrier collection with the contacting area varying between 4 and 5% (to minimize contact area between CIGS and Mo) [6].

The final bandgap of the material depends on the Ga content in the cell [7]. But, if the [Ga]/[Ga] + [In] (GGI) ratio is > 0.3, the performance of the device degrades, limiting the maximum achievable V_{OC} for the device [8]. Recently, the addition of silver (Ag) in a CIGS solar cell has gained greater interest; it reduces the defect density, lowers the structural disorder and increases the open circuit voltage for higher bandgap absorber layers [9]. Thus, in this research, an attempt was made to 1) implement a rear interface passivation layer and 2)
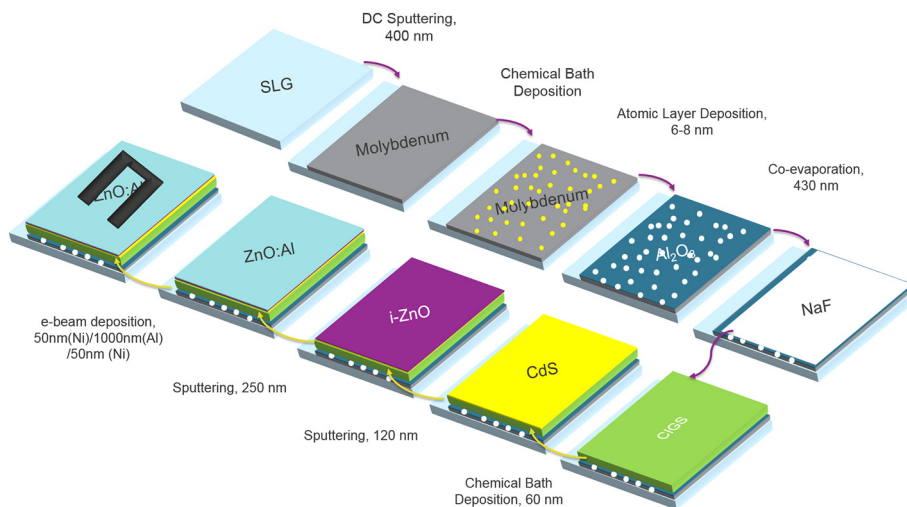
Fig. 1. The various steps involved in the fabrication of a passivated CIGS device. A 1-stage co-evaporation process is used for the absorber deposition.

introduce silver into the absorber of a passivated cell. The results of passivated device and the silver incorporated passivated device are discussed and compared to a reference solar cell.

2. Experimental details

A substrate configuration was used for cell fabrication (Fig. 1). The Al_2O_3 layer was grown (using atomic layer deposition (ALD)) on a particle rich-cadmium sulfide (CdS) layer and subsequently, the particles were removed from the surface to create the point openings. The reason for choosing CdS nano-particles (NPs) is twofold 1) CdS is used as the buffer layer in the cell, hence the same chemical bath deposition solution can be used (cost saving) 2) the particle size varies from 200 nm to 500 nm, more or less the optimal size required in this case. Post ALD, particle removal was done in many ways such as i) dil. HCl immersion and ii) ultrasonic agitation (Fig. 2). For ALD deposited Al_2O_3 layers thicker than 8 nm, particle removal was unsatisfactory. The highly conformal and self-limiting nature of ALD reactions means that the CdS particles embedded in very thick Al_2O_3 layers are irremovable. Thus, an ultra-thin 6 ± 1 nm layer of Al_2O_3 was deposited to tackle two issues 1) blistering [10] and 2) unsatisfactory particle removal.

For the silver passivated CIGS devices, an ultra-thin layer (~15 nm) of silver was evaporated on to the Mo/CIGS interface and then annealed at 375 °C in a nitrogen environment for roughly 30 min. Silver nanoparticles are created as a result, with the average particle size being 550 ± 20 nm. The idea to use silver NPs comes from Yin et al. [11] who reported that silver NPs at the rear surface of the cell (at the Mo/CIGS interface) tend to diffuse into the CIGS absorber during the high temperature deposition process. The steps involved in the fabrication of the passivated device is given in Table 1.

3. Results and discussion

3.1. Passivated thin-CIGS solar cell

To study the effects of the suggested rear surface modifications (passivation layer and Ag) on device performance, a plain reference, passivated cell and a passivated cell with Ag NPs (Ag passivated) at the rear surface were all fabricated in a single run; the molybdenum, absorber, buffer layer and front contacts are all deposited in the same run. Soda lime glass substrates used in this research had an alkali barrier layer. Hence, to counter this and avoid the so called 'roll over' effect [12], an ultra-thin sodium fluoride ((NaF), (3–4 nm)) layer is deposited pre-CIGS deposition (note, this is done for all the devices). In all cases, a 430 nm CIGS absorber was used with the GGI ratio being 0.29 ± 0.1.

In every device, about 28 cells (32 cells per device, each $0.5 \, cm^2$) were electrically characterized. The statistical results for V_{OC}, fill factor (FF) and efficiency (η) are summarized in Table 2 (shunted cell results were discarded). The above table shows that there is an improvement in the electrical performance of the passivated device when compared to the reference. For the reference device, the average value of efficiency was 7.2% whereas, for the passivated device it was 8.5%, an improvement of 1.3% abs. On average, a 65 mV improvement in the open-circuit voltage was recorded for the passivated device, with the highest recorded V_{OC} value being 604.4 mV. Using conductance-voltage measurements, the doping concentration was calculated and found to be similar for both the devices; $1.9 \times 10^{16} \, cm^{-3}$ for the reference device and $1.1 \times 10^{16} \, cm^{-3}$ for the passivated device. Thus, the rational reason for an improved V_{OC} would be improved rear-surface passivation and reduced surface recombination velocity due to the Al_2O_3 layer. Remarkably, the fill factors for the passivated are acceptable and in
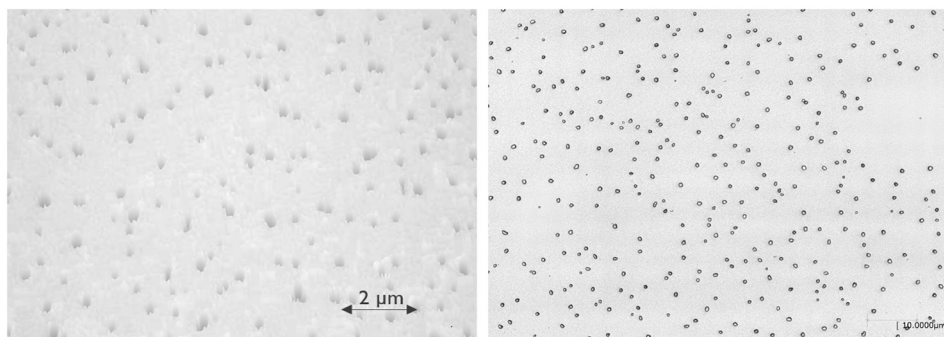

Fig. 2. Optical Microscopy images of 1) point contacts post CdS removal and 2) Ag NP post annealing.

Table 1
Overview of all the steps required for the fabrication of the different CIGS devices used. Note that V stands for the process being carried out and X meaning the process not being carried out.

Sr.	Process description	Reference	Passivated	Ag (passivated)
1	Mo/Soda lime glass (with alkali barrier) cleaning	V	V	V
2	Ultra-thin Ag layer; thermal evaporation	X	X	V
3	Ag nano-particles, annealing at 375 °C	X	X	V
4	Particle rich CdS deposition, CBD	X	V	V
5	Al_2O_3 deposition; ALD (~7 nm)	X	V	V
6	CdS particle removal, point openings	X	V	V
7	NaF layer deposition (3-4 nm)	V	V	V
8	CIGS, 1-stage co-evaporation (no Ga grading) (430 nm)	V	V	V
9	Buffer layer (CdS), CBD (50 nm)	V	V	V
10	Window layer, RF sputtering	V	V	V
11	Ni/Al/Ni front contact, evaporation	V	V	V

fact, higher when compared to the reference cells; 62.1% for the passivated device when compared to 59.4% for the reference. Good fill factors indicate a well-defined and nearly optimized contact area in contrast to low FF values, which together with a high series resistance, is indicative of non-optimized electrical contacts. A relatively low average series resistance of 1.3 Ωcm^{-2} (calculated using one-diode model developed by Hegedus et al. [13]) and high FF for the passivated device suggests that random-nano patterned Al_2O_3 layer in terms of spacing and density, creates a proper and well-defined contacting area. The low series resistance also means that the carrier collection is not deeply affected by the large lateral distance needed by the charge carrier to reach the point contacts [14]. Furthermore, for an increased open-circuit voltage, the FF is expected to improve [14].
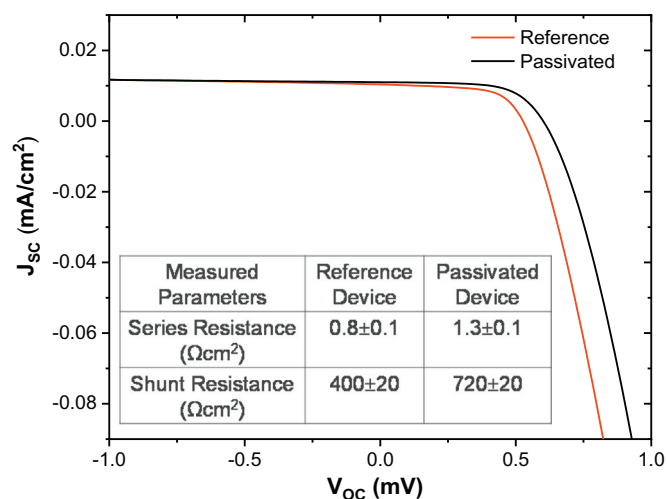
Both the devices have good-diode like behavior (from the dark JV curve not shown here) however, the reference device appeared to be slightly shunted (from the illuminated JV curve, Fig. 3). The dark JV curve of the reference cell does not show any sign of shunting; the reference cells are affected by voltage-dependent current collection [14]. For thin-film solar cells with shorter diffusion lengths and higher absorption coefficients like CIGS, the current generation has a greater reliance on the electric field assisted drift [14]. Thus, the photo-current decreases with decreasing field or increasing forward bias. Lower diffusion lengths can be attributed to either higher bulk and/or rear interface recombination [10]. The same is not observed for the passivated device, hinting a reduced interface recombination (bulk remains the same in both the cases). Higher charge carrier life time is also observed for the passivated device (from TR-PL measurements, not shown here), and in the present case, the bulk remains unchanged. Hence it is attributed to passivating qualities of the Al_2O_3 layer.

Sufficiently good V_{OC} (> 530 mV) and decent FF (> 59%) were obtained, however the efficiency was limited by the low J_{SC} values (< 24 mAcm^{-2}) in both the devices. Yet, when compared to the reference device, a slight improvement in the average J_{SC} was observed (+ 0.2 mAcm^{-2}). For the passivated solar cell, a part of the light in the near infra-red region is reflected at the Al_2O_3/Mo interface into the CIGS absorber by light interference fringes. However, the reflection is stronger for thicker Al_2O_3 layers, thus, only a marginal improvement in the J_{SC} (Fig. 4) was obtained in the present research. This would suggest that the enhanced J_{SC} is not only due to optical improvements but also due the electronic effects of the passivation layer. Therefore, explanations for the improved J_{SC} could be: 1) reduced rear interface trap

Fig. 3. Representative illuminated JV curves for the reference and passivated devices. From the illustration, it is noted that 1) for the passivated device the open circuit voltage is increased 2) the reference device is shunted, effecting its fill factor.

density leading to a lower surface recombination velocity [10] 2) higher minority charge carrier diffusion length due to an induced electric field caused by the Al_2O_3 layer [15] and 3) improved reflection of light into absorber [14].

3.2. Passivated Ag-CIGS solar cells

For an Al_2O_3 passivated (rear) CIGS device, contacts are needed for efficient carrier collection. In the previous case, the CdS NPs used to create the contacts were removed from the surface. In this case however, it is necessary that the Ag particles remain on the surface. Thus, initially, the ALD deposition parameters were varied drastically to try and obtain non-conformal ALD growth. In doing so, it is possible that some regions of the cell or regions around complex 3-D structures (like the nano-particles) not be uniformly coated. The idea for non-conformal ALD growth can be explained as follows; in an idealized temperature window for ALD depositions, the growth per cycle (GPC) is weakly

Table 2
Statistical results for 25 randomly characterized solar cells under AM 1.5 spectrum, with each cell being 0.5 cm^2 in area. Both the reference and the passivated devices were deposited in the same run, have a thickness of about 430 nm with a constant GGI ratio of 0.29 $\pm$ 0.1.

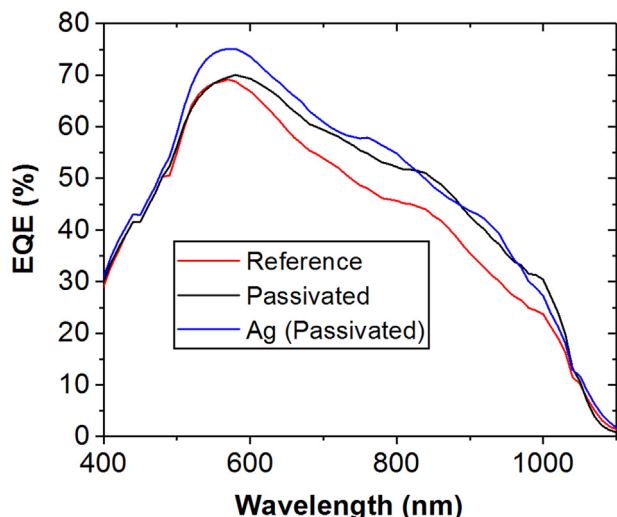| Device	V_{OC} (V)	J_{SC} (mA/cm^2)	FF (%)	Efficiency (%)	Saturation current density (Acm^{-2})
Reference	532 ± 05	22.7 ± 0.4	59.4 ± 0.5	7.2 ± 0.1	2.2×10^{-6}
Passivated	597 ± 07	22.9 ± 0.3	62.1 ± 2	8.5 ± 0.6	1.4×10^{-8}
Ag (Passivated)	560 ± 07	23.3 ± 0.3	60.1 ± 2	7.8 ± 0.6	6.4×10^{-7}

Fig. 4. Representative EQE spectra for the best efficiency cell of the respective devices.

dependent on the temperature. However, outside that temperature window, the idealized ALD behavior can be lost due to the following reasons i) condensation: precursor gases can condense on the substrate surface which could prevent efficient purging [16] ii) lower temperature: limits completion of precursor reactions due to lack of sufficient reactivity and iii) desorption: the deposited film or the precursor gases may desorb from the surface, effecting the GPC [17]. Thus, an initial trial was made with an extremely thin non-conformal (non-conformal parameters like low temperature (from 150 °C to 100 °C), reducing pulse time for the TMA precursor (from 0.016 to 0.006 s) etc.) Al_2O_3 layer (5 nm) grown on the silver NPs. With these parameters, a thin-CIGS device was fabricated. By analyzing the results, it was absorbed that extremely low short circuit current (11 mA/cm^2), high series resistances and extremely low shunt resistances were obtained (about 9 Ωcm^2 and 33 Ωcm^2 respectively). The high series resistance and poor carrier collection suggests that the contacts were not well defined or created properly. Also, it is difficult to conclude if the contacts were a result of the non-conformal ALD or the pre-deposited NaF layer (currently under research). Thus, non-conformal ALD cannot be used as a controllable and repeatable method to create contacts. A different approach was tested to create contacts and keep the Ag NPs on the surface; to use of CdS NPs to create the contacts as explained in Table 1. The results of same are summarized in Table 2.

From Table 2, it is possible to see that there is an improvement in the open-circuit voltage (+28 mV when compared to the reference), yet the increase is not as high as in the case of a plain passivated device. The reduced open-circuit voltage can partially be explained by the lower doping concentration in the Ag-CIGS device (in the range of 10^{15} cm^{-3}), even lower than what was obtained for the plain passivated device. The FF was also reduced when compared to the plain passivated device; an average of 60.1% was obtained. This could be due to the CdS removal step; during the CdS nano-particle removal, even silver nano-particles could have partially been removed from the surface. Thus, the electrical contact area is increased and/or not optimized, which effects the fill factor.

An important trend observed in the present case is the slight improvement in the short circuit current (+0.6 mA/cm^2). The improvement in the short circuit current can also be seen in the external quantum efficiency (EQE) curves (Fig. 4), where there is an improvement in the entire solar spectrum. Therefore, explanations for the improved J_{SC} could be due the combined effects of the passivation layer, the reduced disorder/defects in the CIGS structure due partial silver addition (hence an improved EQE spectra in the visible light region)

and light scattering of the Ag NPs. However, further studies are needed to confirm the same. This is because silver has a low diffusion coefficient, hence higher temperatures are required to promote silver diffusion in the absorber [18,19]. Since, in the present case, the CIGS deposition conditions were not varied significantly (for example the deposition temperature remained unchanged), it is more likely that the silver did not or partially diffused into the absorber (due to reduced CIGS absorber thickness). This possibly explains the reasonable shunt resistances obtained from the device. Moreover, for obtaining high quality Ag-CIGS devices, the uniformity of Ag in the absorber is essential, which in this case couldn't have been achieved. Consequently, moderate efficiencies were obtained (on average 7.8%) owing to the marginal improvements in the FF, J_{SC} and V_{OC}. The PL spectrum of the Ag-CIGS device was amplified when compared to the reference, however, it is more likely that it is a result of the passivation layer and not the Ag. Besides, there is no significant increase in the bandgap of the Ag-CIGS device (observed from both the photoluminescence spectra (not shown here) and the EQE) further proof of the lack of silver in the absorber. However, it must be noted that this was an initial trial made on such devices more and optimization studies are being researched actively.

4. Conclusions

In summary, an advanced architecture to integrate a rear surface passivation scheme in a thin-CIGS solar device was demonstrated. The modified rear surface consisted of an ultra-thin passivation layer with nano-sized point openings on its surface. A simple and technologically feasible method was demonstrated to generate nano-sized point openings without effecting the fill factor severely. Implementing Al_2O_3 passivation schemes impacts the cell performance positively; i) it reduces the rear interface defects ii) it lowers the rear interface recombination and iii) it improves the minority carrier diffusion lengths. Higher efficiencies were obtained owing to higher fill factors and open-circuit voltages, bringing down the efficiency losses when compared to a standard thin-CIGS device. Furthermore, an attempt was made to introduce silver into the absorber, however, more research and studies are needed in that aspect of the cell.

Acknowledgements

References

[1] B. Vermang, V. Fjällström, X. Gao, M. Edoff, Improved rear surface passivation of Cu (In, Ga) Se2 solar cells: a combination of an Al 2O3 rear surface passivation layer and nanosized local rear point contacts, IEEE J. Photovolt. 4 (1) (2014 Jan) 486–492.

[2] T. Plamena, Solar Frontier Reaches 22.9% Efficiency on Thin-Film CIS Cell, Available: https://renewablesnow.com/news/solar-frontier-reaches-229-efficiency-on-thin-film-cis-cell-595223/.

[3] R. Kotipalli, O. Poncelet, G. Li, Y. Zeng, L.A. Francis, B. Vermang, D. Flandre, Addressing the impact of rear surface passivation mechanisms on ultra-thin Cu (In, Ga) Se2 solar cell performances using SCAPS 1-D model, Sol. Energy 157 (2017 Nov 15) 603–613.

[4] W.W. Hsu, J.Y. Chen, T.H. Cheng, S.C. Lu, W.S. Ho, Y.Y. Chen, Y.J. Chien, C.W. Liu, Surface passivation of Cu (In, Ga) Se2 using atomic layer deposited Al2O3, Appl. Phys. Lett. 100 (2) (2012 Jan 9) 023508.

[5] R. Kotipalli, B. Vermang, J. Joel, R. Rajkumar, M. Edoff, D. Flandre, Investigating the electronic properties of Al2O3/Cu (In, Ga) Se2 interface, AIP Adv. 5 (10) (2015 Oct) 107101.

[6] B. Vermang, H. Goverde, L. Tous, A. Lorenz, P. Choulat, J. Horzel, J. John, J. Poortmans, R. Mertens, Approach for Al2O3 rear surface passivation of industrial p-type Si PERC above 19%, Prog. Photovolt. Res. Appl. 20 (3) (2012 May) 269–273.

[7] R. Kotipalli, B. Vermang, V. Fjällström, M. Edoff, R. Delamare, D. Flandre, Influence of Ga/(Ga+ In) grading on deep-defect states of Cu (In, Ga) Se2 solar cells, Phys. Status Solidi 9 (3) (2015 Mar) 157–160.

[8] S.H. Wei, S.B. Zhang, A. Zunger, Effects of Ga addition to CuInSe 2 on its electronic, structural, and defect properties, Appl. Phys. Lett. 72 (24) (1998 Jun 15)

3199–3201.

[9] K. Yamada, N. Hoshino, T. Nakada, Crystallographic and electrical properties of wide gap Ag (In 1−x, Ga x) Se2 thin films and solar cells, Sci. Technol. Adv. Mater. 7 (1) (2006 Jan) 42.

[10] B. Vermang, V. Fjällström, J. Pettersson, P. Salomé, M. Edoff, Development of rear surface passivated Cu (In, Ga) Se 2 thin film solar cells with nano-sized local rear point contacts, Sol. Energy Mater. Sol. Cells 117 (2013 Oct 31) 505–511.

[11] G. Yin, A. Steigert, P. Andrae, M. Goebelt, M. Latzel, P. Manley, I. Lauermann, S. Christiansen, M. Schmid, Integration of plasmonic Ag nanoparticles as a back reflector in ultra-thin Cu (In, Ga) Se2 solar cells, Appl. Surf. Sci. 355 (2015 Nov 15) 800–804.

[12] B. Vermang, J.T. Wätjen, V. Fjällström, F. Rostvall, M. Edoff, R. Kotipalli, F. Henry, D. Flandre, Employing Si solar cell technology to increase efficiency of ultra-thin Cu (In, Ga) Se2 solar cells, Prog. Photovolt. Res. Appl. 22 (10) (2014 Oct) 1023–1029.

[13] S.S. Hegedus, W.N. Shafarman, Thin-film solar cells: device measurements and analysis, Prog. Photovolt. Res. Appl. 12 (2–3) (2004 Mar) 155–176.

[14] P.M. Salomé, B. Vermang, R. Ribeiro-Andrade, J.P. Teixeira, J.M. Cunha, M.J. Mendes, S. Haque, J. Borme, H. Águas, E. Fortunato, R. Martins, Passivation of interfaces in thin film solar cells: understanding the effects of a nanostructured rear point contact layer, Adv. Mater. Interfaces 5 (2) (2018 Jan) 1701101.

[15] B. Vermang, J.T. Wätjen, C. Frisk, V. Fjällström, F. Rostvall, M. Edoff, P. Salomé, J. Borme, N. Nicoara, S. Sadewasser, Introduction of Si PERC rear contacting design to boost efficiency of Cu (In, Ga) Se 2 solar cells, IEEE J. Photovolt. 4 (6) (2014 Nov) 1644–1649.

[16] H.B. Profijt, Plasma-Surface Interaction in Plasma-Assisted Atomic Layer Deposition, Doctoral dissertation, PhD thesis Eindhoven University of Technology, 2012.

[17] H.B. Profijt, P. Kudlacek, M.C. Van de Sanden, W.M. Kessels, The influence of ions and photons during plasma-assisted ALD of metal oxides, ECS Trans. 33 (2) (2010 Oct 1) 61–67.

[18] Z. Xianfeng, T. Kobayashi, Y. Kurokawa, A. Yamada, Growth of Ag (In, Ga) Se2 films by modified three-stage method and influence of annealing on performance of solar cells, Jpn. J. Appl. Phys. 51 (10S) (2012 Oct 22) 10NC05.

[19] X.F. Zhang, M. Kobayashi, Study on growth process of Ag (In Ga) Se2 films by a three-stage co-evaporation method using molecular beam epitaxy apparatus, IEEE Photon. J. 9 (2017 Mar) 8400109.